Hindawi Publishing Corporation
International Journal of Photoenergy
Volume 2013, Article ID 649540, 6 pages
http://dx.doi.org/10.1155/2013/649540

Research Article

Bulky Macroporous TiO_2 Photocatalyst with Cellular Structure via Facile Wood-Template Method

Qingfeng Sun,[1,2] Yun Lu,[1] Jinchun Tu,[3] Dongjiang Yang,[4] Jun Cao,[2] and Jian Li[1]

[1] *Material Science and Engineering College, Northeast Forestry University, Harbin 150040, China*
[2] *College of Mechanical and Electrical Engineering, Northeast Forestry University, Harbin 150040, China*
[3] *Key Laboratory of Tropical Biological Resources of Ministry of Education, College of Materials and Chemical Engineering, Hainan University, Haikou 570228, China*
[4] *College of Chemistry, Chemical and Environmental Engineering, Qingdao University, Qingdao 266071, China*

Correspondence should be addressed to Jun Cao; zdhcj@126.com and Jian Li; jianli@nefu.edu.cn

Received 20 January 2013; Revised 14 March 2013; Accepted 15 March 2013

Academic Editor: Elias Stathatos

We report a bulky macroporous TiO_2 particles with cellular structure prepared in the presence of wood slices as template. Firstly, TiO_2 sol was coated onto the wood slices by repeated dip-coating process. Then, after calcinations at 550°C, the wood template could be removed, and the bulky TiO_2 structure was obtained. The prepared samples were characterized by scanning electron microscopy (SEM), X-ray diffraction (XRD), energy dispersive spectroscopy (EDS), and transmission electron microscope (TEM) techniques. XRD pattern confirmed the crystalline phase of the wood-templated TiO_2 is anatase phase. And interestingly, from the observation of SEM image, the wood-templated TiO_2 inherited the initial cellular structures of birch lumber (*B. albosinensis Burk*), and numerous macropores were observed in the sample. Meanwhile, the wood-templated TiO_2 presented a superior photocatalytic ability to decompose Rhodamine B (RhB) under ultraviolet irradiation.

1. Introduction

Template-directed synthesis is currently one of the most widely used methods for fabricating inorganic materials on account of its facility and versatility [1–4]. In addition to some artificial templates like latex particles [5], polymer foams [6], ion-exchange resins [7], and carbon fibers [8], many natural templates have been attracted to much attention for constructing a number of inorganic materials. The natural species utilized as templates for the formation of inorganic materials are available from bacterial superstructures [9], insect wings [10], wool and cotton/cloth textile [11], diatoms [12], dog and human hair [13], living cells [14], mushroom gills [13], plant leaves [10], paper [15], pollen grains [16], shell membrane [17], silk fiber [13], skeletal plates [18], spider silk [8, 10], and wood [19–24]. These materials from nature combine many inspiring properties, such as sophistication, miniaturization, hierarchical organizations, hybridization, resistance, and adaptability, after billions of years of stringent selection processes [4]. From the research results, using natural species as template for building inorganic materials is an effective strategy to obtain morphology controllable materials with structural specialty, complexity, and related unique properties.

Among these natural templates, wood is a naturally grown composite material possessing complex hierarchical cellular and pit structures that are comprised principally of biopolymers, mainly cellulose, hemicellulose, and lignin [25, 26]. The wood vessels and fibers are hollow tubes, and the arrangement of these vessels and fibers varies considerably different with different wood species. The cellular structural hierarchy of wood ranges from the millimeter scale of the growth ring and longitudinal tracheid, the micrometer scale of the cell wall and diameter, to the nanometer scale of the molecular fiber and membrane structure of the cell wall. The open porosity is accessible for liquid or gaseous infiltration [3, 20]. These features of wood make it a perfect candidate as a template for generating porous inorganic materials with both structural and morphological complexities. Previously some efforts have been made

toward transforming wood cellular structures into inorganic SiC [27, 28], TiC [29], and macroporous zeolites [20]. By impregnating the wood templates with metal alkoxide solutions and applying standard sol-gel chemistry, various metal oxide porous materials, such as TiO_2 [30], Al_2O_3 [31], Fe_2O_3 [21], and Cr_2O_3 [32], have been produced using this approach.

In these inorganic materials, TiO_2 is one of the most promising functional materials and extensively used in photocatalysis [33, 34], solar cells [35], and paints [36] because of its superior chemical stability and nontoxicity [37, 38]. TiO_2 exists mainly in four polymorphs in nature, anatase (tetragonal, space group $I4_1/amd$), rutile (tetragonal, space group $P4_2/mnm$), brookite (orthorhombic, space group $Pbca$), and TiO_2(B) (monoclinic, space group $C2/m$) [39–42]. In photocatalytic study, anatase TiO_2 is generally considered to be more active than rutile crystalline [43]. Moreover, anatase TiO_2 with higher crystallinity is preferred for photocatalysis, since higher crystallinity means fewer defects for the recombination of photogenerated electrons and holes [36]. In the current research, different kinds of TiO_2 nanomaterials like nanoparticles, nanosheet, nanotube, or nanofiber have been fabricated using different method. However, TiO_2 with wood structures has been seldom reported.

To this purpose, we developed an efficient pathway to synthesize wood-templated TiO_2. The morphology, chemical compositions, and crystalline phase of the prepared TiO_2 were characterized by SEM, EDS, HRTEM, and XRD, respectively. Furthermore, the photocatalytic activity of the wood-templated TiO_2 was measured under UV irradiation.

2. Materials and Method

2.1. Raw Materials. All the chemicals were supplied by Shanghai Boyle Chemical Co. Ltd. and used as received. The air-dried birch lumber (*B. albosinensis Burk*) was cut into slices with a size of 20 mm (tangential) × 20 mm (radial) × 2 mm (longitudinal). The wood slices were pretreated in a Soxhlet apparatus with 95% ethanol at 80°C for 6 h under reflux to remove the extracts like the fats and fatty acids in the wood. Then these slices were rinsed with deionized water. Finally, the treated wood slices were vacuumly dried at 60°C for over 24 hours.

2.2. Preparation of TiO_2 Sol. Tetrabutylorthotitanate (TBOT), diethanolamine (DEA), and absolute ethanol were used as starting materials. The 34 mL of TBOT and 11 mL of DEA were dissolved in 100 mL ethanol to prepare the precursor solution. After stirring for 2 h at room temperature, a mixed solution of 55 mL water and 9 ml ethanol was dropwise added following stirred another 3 h. Then TiO_2 sol was obtained.

2.3. Fabrication of Wood-Templated TiO_2. Firstly, wood slices were coated by TiO_2 sol through a repeated dip-coating process. The pretreated wood slices were immersed into the as-prepared TiO_2 sol for 5 min. After that, these slices were dried at 80°C for 3 h. This process was repeated for 5 times to ensure TiO_2 sol densely and evenly covered onto the wood slices. Then, calcination process was employed to remove the wood template. To get wood-templated TiO_2, wood coated by TiO_2 sol was calcined in a muffle furnace at the temperature of 550°C for 3 h in air atmosphere and air cooled to room temperature. Finally, the calcined samples were taken out from the muffle furnace, and the wood-templated TiO_2 was obtained.

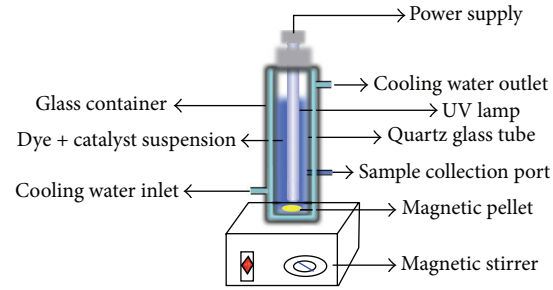

Figure 1: The schematic diagram of the photocatalytic reactor.

2.4. Characterizations. The morphology of the samples was observed by scanning electron microscopy (SEM, FEI, Quanta 200) and transmission electron microscopy (TEM, FEI Tecnai F20). The chemical compositions of the untreated and treated wood were measured by energy dispersive spectroscopy (EDS, attached to the SEM). The crystalline structures were identified by X-ray diffraction (XRD, Rigaku, D/MAX 2200) operating with Cu Kα radiation ($\lambda = 1.5418$ Å) at a scan rate (2θ) of 4°/min with an accelerating voltage of 40 kV and an applied current of 30 mA ranging from 10° to 70°.

2.5. Evaluation of Photocatalytic Activity. The photocatalytic activity of the samples was estimated through the decomposition of Rhodamine B (RhB) in a reactor with a volume of 100 mL. The irradiation source was an ultraviolet 100 W lamp (Shanghai Rongbo Co., China) with a wavelength of 254 nm. The photocatalytic activities of the prepared products were judged by measuring the loss of RhB in aqueous solution. A suspension involving 100 mg of catalyst and 100 mL RhB solution with an original concentration of 50 mg/L was magnetically stirred on the dark for 1 h without interrupting before irradiation. The change of solution concentration in every 30 min was measured to judge the absorbability of catalysts in the dark. At every interval during the process of 3 h, a certain sample of the mixture was collected, centrifuged, and then measured. The degradation rate for denoting the degradation efficiency of RhB was obtained by measuring the change in absorbance on a UV-Vis spectrophotometer (TU-190, Beijing Purkinje, China), and its maximum absorption wavelength of RhB was 554.5 nm. The schematic diagram of the photocatalytic reactor was represented in Figure 1.

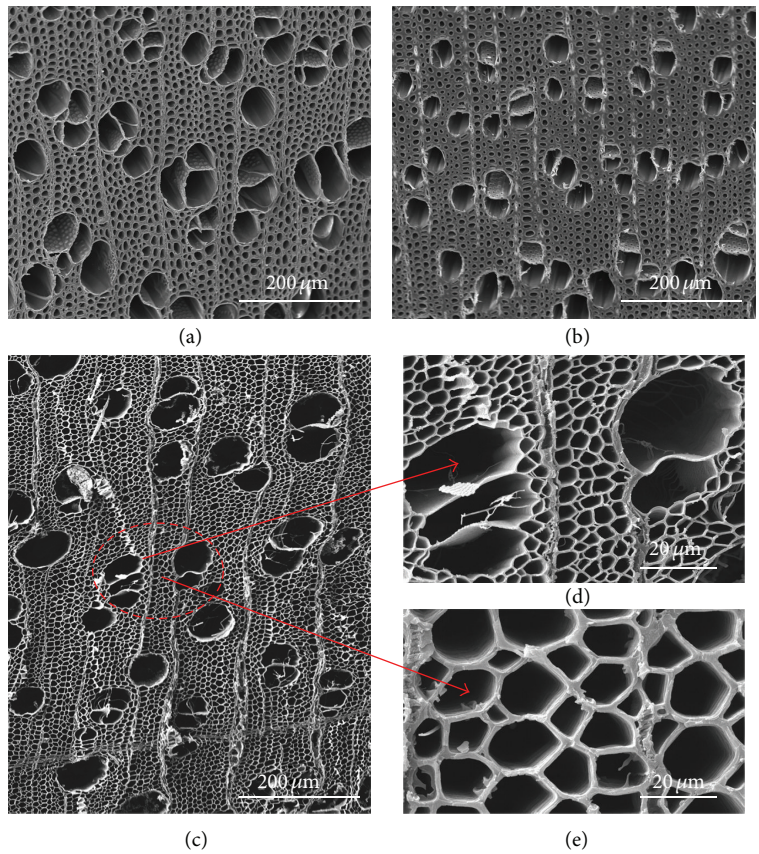

FIGURE 2: SEM images of the cross-section of (a) the original wood, (b) the wood coated by TiO_2 sol, (c) wood-templated TiO_2, (d) the magnified calcined wood vessels, and (e) the magnified calcined wood fibers, respectively.

3. Results and Discussion

Figure 2 showed the morphologies of the cross-section of the original wood, wood coated by TiO_2 sol, and wood-templated TiO_2, respectively. As shown in Figure 2(a), the cellular structures of the original wood could be clearly observed. The wood vessels with the diameter of about 20~50 μm are irregular circular. The wood fibers with the diameter of about 5~20 μm are uniformly arranged among the wood vessels. In Figure 2(b), the wood structure has not obviously changed after the dip-coating process by TiO_2 sol. It can be clearly seen from the Figure 2(c) that the structures of the original wood were commendably remained after the calcined process. In the magnified SEM image (Figure 2(d)), calcined wood vessels with a little collapse could be obviously observed with the diameter of about 35 μm. Simultaneously, the calcined wood fibers shown in Figure 2(e) with a thinner cellular wall compared to the original wood were well arranged without any collapse. The diameters of these fibers are about 15 μm. In a word, TiO_2 with the wood cellular structure was successfully prepared by dip-coating and calcination process. The microscopic structures of the original wood could not be destroyed with the previous process.

EDS spectra were also recorded for the original wood, wood coated by TiO_2 sol, and wood-templated TiO_2, respectively. As shown in Figure 3(a), the carbon, oxygen, and gold elements could be detected from the EDS spectrum of the original wood. The elements of carbon and oxygen are originated from the wood substrate, and the element of gold is from the coating layer used for SEM observation. Besides the signal of carbon and oxygen elements, titanium and nitrogen elements were displayed in the spectrum of TiO_2 sol-coated wood slices (Figure 3(b)). The elements of titanium and nitrogen are stemmed from TBOT and DEA in the TiO_2 sol, respectively. After calcination at 550°C, only oxygen and titanium elements could be probed from the EDS spectrum (Figure 3(c)), and no other elements were detected which confirmed that the components of the original wood and the TiO_2 precursor were completely removed during the calcination process.

XRD patterns of the original wood, the wood coated by TiO_2 sol, and wood-templated TiO_2 were presented in Figure 4. Figure 4(a) revealed a typical XRD pattern of the original wood. The diffraction peaks at 16° and 22.6° were believed to represent the crystalline region of the cellulose in wood [25]. In Figure 4(b), no other new diffraction peaks were founded except for the diffractive characteristics of the initial wood, which might be due to that the crystal phase of TiO_2 sol is consisted of amorphous TiO_2 before the calcination. Apparently, in Figure 4(c), the diffraction peaks at 16° and 22.6° belonging to the original wood sample disappeared. New strong diffraction peaks were observed

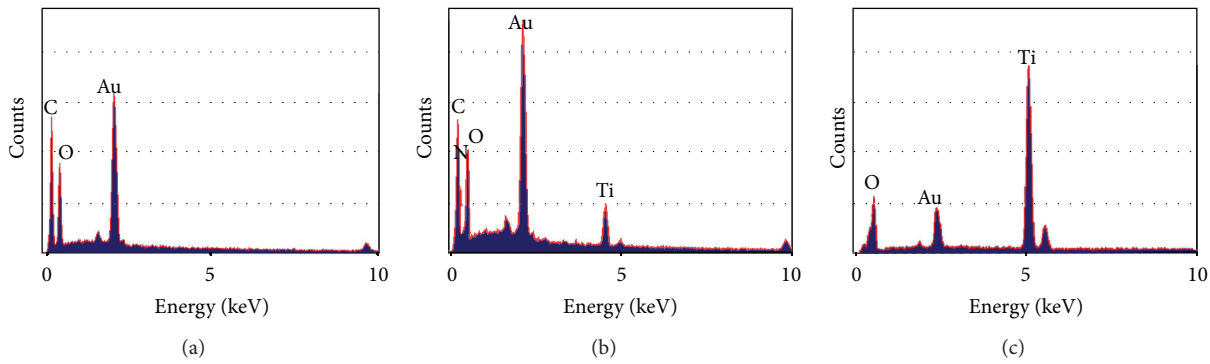

Figure 3: EDS spectra of (a) the original wood, (b) wood coated by TiO_2 sol, and (c) wood-templated TiO_2.

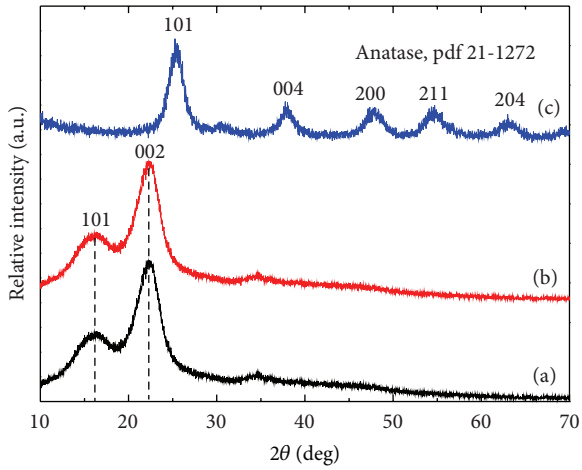

Figure 4: XRD patterns of (a) the original wood, (b) the wood coated by TiO_2 sol, and (c) wood-templated TiO_2.

for the calcined sample, which indicated the formation of new crystal structures of the calcined wood sample. As shown in pattern of wood-templated TiO_2, the diffraction peaks at 25°, 38°, 48°, and 54° could be assigned to the diffractions of the (101), (004), (200), and (211) planes of anatase TiO_2 (JCPDS number 21-1272) [36, 40], respectively. XRD pattern of the wood-templated TiO_2 also confirmed that the components of the pristine wood were completely got rid of through the calcination process.

TEM images in Figure 5(a) revealed a much more fine structure of the obtained TiO_2 sintered at 550°C for 3 h. Though TiO_2 sample has been pulverized, the slices were found in the TEM image, just like the cellular framework of the original wood. Consequently, we could safely conclude that the cellular structure of the original wood has been preserved after the calcination process. The selected area electron diffraction (SAED) of the slice in Figure 5(b) illuminated the crystalline phase of the wood-templated TiO_2 is polycrystalline with the coexistence of the diffraction rings and spots at the SAED pattern. The HRTEM image in Figure 5(c) revealed that the distance between the adjacent lattice fringes of (101) planes is about 0.352 nm which is corresponding to the anatase TiO_2 crystal (a = 0.325 nm, c = 0.521 nm).

The photocatalytic ability of the obtained cellular-structured TiO_2 was investigated by decomposing RhB dye, a very difficult degradable and highly toxic organic pollutant. The photodegradation curves of RhB were exhibited in Figure 6. The wood-templated TiO_2 could photodegrade the RhB under UV light irradiation. The original wood shown in Figure 6(a) had a little photocatalytic activity of about 4.6% on RhB. It was mainly ascribed to the physical absorption effect because of porous wood. In Figure 6(b), the wood coated by TiO_2 sol showed a photocatalytic activity of about 8.21% on RhB. However, wood-templated TiO_2 expressed a superior photocatalytic activity of about 92.5% on RhB (Figure 6(c)). The photocatalytic efficiency of the obtained TiO_2 was greatly enhanced probably, since the prepared TiO_2 remained the original wood cellular structures. The original wood porous structure could be affording a portable carrier for absorbing and degrading much organic pollutants.

Meanwhile, the photocatalytic activity of wood-templated TiO_2 was compared to the commercially available TiO_2 P25 (Degussa, Germany) that consist of both anatase (80%) and rutile (20%) phases of TiO_2. The same experimental conditions were selected for P25. From the comparison between catalysts wood-templated TiO_2 and P25 (Figure 6(d)), it can be seen that RhB underwent decomposition of a little faster in the case of the latter catalyst. But the problem with the P25 powder is that the TiO_2 disperses in water forming a white colloidal solution, and it is difficult to separate from the reaction mixture for reuse. The separation performance test showed that the wood-templated TiO_2 has a good sedimentation ability and can decanted from the suspension in about 15 min, while the P25 do not decant after 45 min.

4. Conclusions

In the present paper, the anatase wood-templated TiO_2 was successfully fabricated by using a facile dip-coating and subsequent calcination process. The as-prepared TiO_2 possessed the typical cellular structure with unbroken vessels and uniformly arranged wood fibers. Also, this wood-templated TiO_2 presented a superior photocatalytic degradation of RhB.

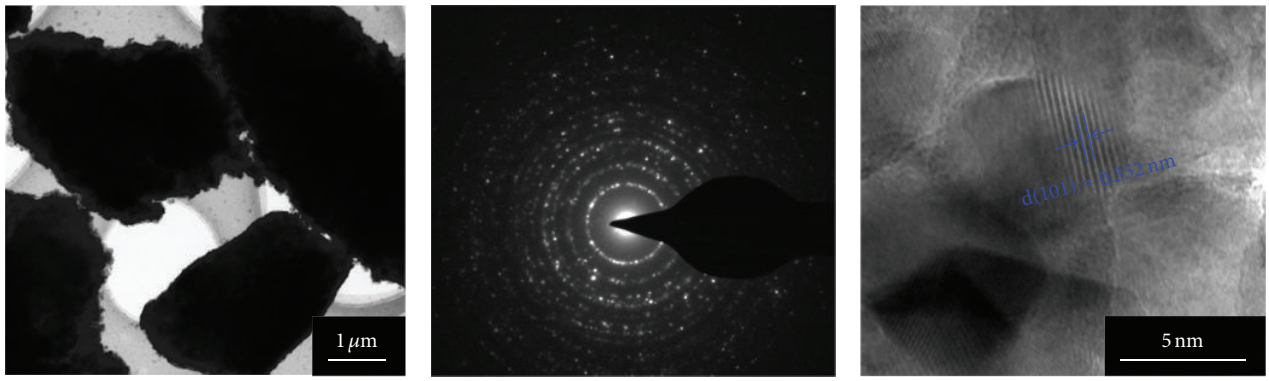

FIGURE 5: (a) TEM images, (b) the selected electron diffraction patterns, and (c) HRTEM images of the wood-templated TiO_2.

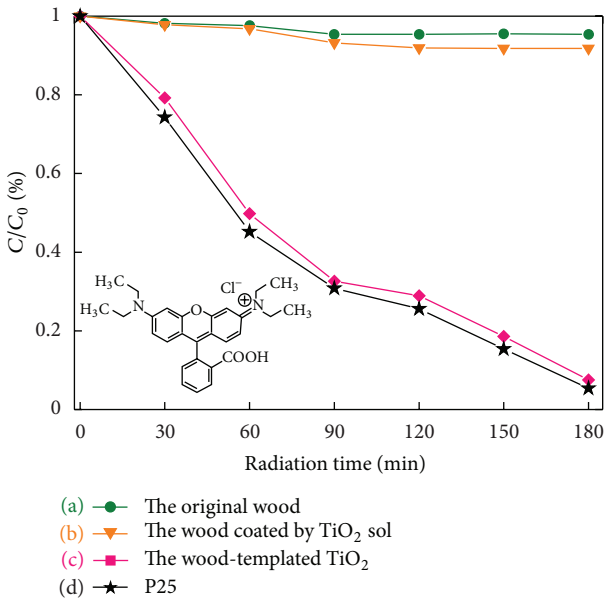

FIGURE 6: Photocatalytic activity of (a) the original wood, (b) the wood coated by TiO_2 sol, (c) the wood-templated TiO_2, and (d) P25, respectively.

This paper probably provided another way for fabricating inorganic materials using the natural wood as template.

Acknowledgments

This work was financially supported by The National Natural Science Foundation of China (Grant nos. 31270590 and 21207073) and National Basic Research Program of China (973 Program, Grant no. 2009CB220000).

References

[1] S. V. N. T. Kuchibhatla, A. S. Karakoti, D. Bera, and S. Seal, "One dimensional nanostructured materials," *Progress in Materials Science*, vol. 52, no. 5, pp. 699–913, 2007.

[2] J. Li, Q. Xu, J. Wang, J. Jiao, and Z. Zhang, "Controlled synthesis of monolithic hierarchical porous materials using wood as a template with assistance of supercritical carbon dioxide," *Industrial and Engineering Chemistry Research*, vol. 47, no. 20, pp. 7680–7685, 2008.

[3] O. Paris, I. Burgert, and P. Fratzl, "Biomimetics and biotemplating of natural materials," *MRS Bulletin*, vol. 35, no. 3, pp. 219–225, 2010.

[4] H. Zhou, T. Fan, and D. Zhang, "Biotemplated materials for sustainable energy and environment: current status and challenges," *ChemSusChem*, vol. 4, no. 10, pp. 1344–1387, 2011.

[5] L. Huang, Z. Wang, J. Sun et al., "Fabrication of ordered porous structures by self-assembly of zeolite nanocrystals," *Journal of the American Chemical Society*, vol. 122, no. 14, pp. 3530–3531, 2000.

[6] Y. J. Lee, J. S. Lee, Y. S. Park, and K. B. Yoon, "Synthesis of large monolithic zeolite foams with variable macropore architectures," *Advanced Materials*, vol. 13, no. 16, pp. 1259–1263, 2001.

[7] L. Tosheva, B. Mihailova, V. Valtchev, and J. Sterte, "Zeolite beta spheres," *Microporous and Mesoporous Materials*, vol. 48, no. 1–3, pp. 31–37, 2001.

[8] Y. J. Wang, Y. Tang, X. D. Wang, W. L. Yang, and Z. Gao, "Fabrication of hollow zeolite fibers through layer-by-layer adsorption method," *Chemistry Letters*, no. 11, pp. 1344–1345, 2000.

[9] S. A. Davis, S. L. Burkett, N. H. Mendelson, and S. Mann, "Bacterial templating of ordered macrostructures in silica and silica-surfactant mesophases," *Nature*, vol. 385, no. 6615, pp. 420–423, 1997.

[10] G. Cook, P. L. Timms, and C. Göltner-Spickermann, "Exact replication of biological structures by chemical vapor deposition of silica," *Angewandte Chemie—International Edition*, vol. 42, no. 5, pp. 557–559, 2003.

[11] H. Imai, M. Matsuta, K. Shimizu, H. Hirashima, and N. Negishi, "Preparation of TiO_2 fibers with well-organized structures," *Journal of Materials Chemistry*, vol. 10, no. 9, pp. 2005–2006, 2000.

[12] M. W. Anderson, S. M. Holmes, N. Hanif, and C. S. Cundy, "Hierarchical pore structures through diatom zeolitization," *Angewandte Chemie—International Edition*, vol. 39, no. 15, pp. 2707–2710, 2000.

[13] Y. Kim, "Small structures fabricated using ash-forming biological materials as templates," *Biomacromolecules*, vol. 4, no. 4, pp. 908–913, 2003.

[14] S. Chia, J. Urano, F. Tamanoi, B. Dunn, and J. I. Zink, "Patterned hexagonal arrays of living cells in sol-gel silica films," *Journal of the American Chemical Society*, vol. 122, no. 27, pp. 6488–6489, 2000.

[15] A. N. Shigapov, G. W. Graham, R. W. McCabe, and H. K. Plummer Jr., "The preparation of high-surface area, thermally-stable, metal-oxide catalysts and supports by a cellulose templating approach," *Applied Catalysis A*, vol. 210, no. 1-2, pp. 287–300, 2001.

[16] S. R. Hall, H. Bolger, and S. Mann, "Morphosynthesis of complex inorganic forms using pollen grain templates," *Chemical Communications*, vol. 9, no. 22, pp. 2784–2785, 2003.

[17] D. Yang, L. Qi, and J. Ma, "Eggshell membrane templating of hierarchically ordered macroporous networks composed of TiO_2 tubes," *Advanced Materials*, vol. 14, no. 21, pp. 1543–1546, 2002.

[18] F. C. Meldrum and R. Seshadri, "Porous gold structures through templating by echinoid skeletal plates," *Chemical Communications*, no. 1, pp. 29–30, 2000.

[19] T. Ota, M. Imaeda, H. Takase et al., "Porous titania ceramic prepared by mimicking silicified wood," *Journal of the American Ceramic Society*, vol. 83, no. 6, pp. 1521–1523, 2000.

[20] A. Dong, Y. Wang, Y. Tang et al., "Zeolitic tissue through wood cell templating," *Advanced Materials*, vol. 14, no. 12, pp. 926–929, 2002.

[21] Z. Liu, T. Fan, W. Zhang, and D. Zhang, "The synthesis of hierarchical porous iron oxide with wood templates," *Microporous and Mesoporous Materials*, vol. 85, no. 1-2, pp. 85–88, 2005.

[22] Z. Liu, T. Fan, and D. Zhang, "Synthesis of biomorphous nickel oxide from a pinewood template and investigation on a hierarchical porous structure," *Journal of the American Ceramic Society*, vol. 89, no. 2, pp. 662–665, 2006.

[23] Z. Liu, T. Fan, D. Zhang, X. Gong, and J. Xu, "Hierarchically porous ZnO with high sensitivity and selectivity to H_2S derived from biotemplates," *Sensors and Actuators B*, vol. 136, no. 2, pp. 499–509, 2009.

[24] Z. Liu, T. Fan, J. Ding, D. Zhang, Q. Guo, and H. Ogawa, "Synthesis and cathodoluminescence properties of porous wood (fir)-templated zinc oxide," *Ceramics International*, vol. 34, no. 1, pp. 69–74, 2008.

[25] J. Li, Y. Lu, D. Yang, Q. Sun, Y. Liu, and H. Zhao, "Lignocellulose aerogel from wood-ionic liquid solution (1-allyl-3-methylimidazolium chloride) under freezing and thawing conditions," *Biomacromolecules*, vol. 12, no. 5, pp. 1860–1867, 2011.

[26] Y. Lu, Q. Sun, D. Yang et al., "Fabrication of mesoporous lignocellulose aerogels from wood via cyclic liquid nitrogen freezing-thawing in ionic liquid solution," *Journal of Materials Chemistry*, vol. 22, no. 27, pp. 13548–13557, 2012.

[27] J. M. Qian, J. P. Wang, and Z. H. Jin, "Preparation and properties of porous microcellular SiC ceramics by reactive infiltration of Si vapor into carbonized basswood," *Materials Chemistry and Physics*, vol. 82, no. 3, pp. 648–653, 2003.

[28] P. Greil, T. Lifka, and A. Kaindl, "Biomorphic cellular silicon carbide ceramics from wood—I: processing and microstructure," *Journal of the European Ceramic Society*, vol. 18, no. 14, pp. 1961–1973, 1998.

[29] B. Sun, T. Fan, and D. Zhang, "Porous TiC ceramics derived from wood template," *Journal of Porous Materials*, vol. 9, no. 4, pp. 275–277, 2002.

[30] J. Huang and T. Kunitake, "Nano-precision replication of natural cellulosic substances by metal oxides," *Journal of the American Chemical Society*, vol. 125, no. 39, pp. 11834–11835, 2003.

[31] C. R. Rambo and H. Sieber, "Novel synthetic route to biomorphic Al_2O_3 ceramics," *Advanced Materials*, vol. 17, no. 8, pp. 1088–1091, 2005.

[32] T. Fan, X. Li, Z. Liu, J. Gu, D. Zhang, and Q. Guo, "Microstructure and infrared absorption of biomorphic chromium oxides templated by wood tissues," *Journal of the American Ceramic Society*, vol. 89, no. 11, pp. 3511–3515, 2006.

[33] M. Anpo and M. Takeuchi, "Design and development of second-generation titanium oxide photocatalysts to better our environment—approaches in realizing the use of visible light," *International Journal of Photoenergy*, vol. 3, no. 2, pp. 89–94, 2001.

[34] A. D. Paola, S. Ikeda, G. Marcì, B. Ohtani, and L. Palmisano, "Transition metal doped TiO_2: physical properties and photocatalytic behaviour," *International Journal of Photoenergy*, vol. 3, no. 4, pp. 171–176, 2001.

[35] C. C. Hu, T. C. Hsu, and L. H. Kao, "One-step cohydrothermal synthesis of nitrogen-doped titanium oxide nanotubes with enhanced visible light photocatalytic activity," *International Journal of Photoenergy*, vol. 2012, Article ID 391958, 9 pages, 2012.

[36] X. Chen and S. S. Mao, "Titanium dioxide nanomaterials: synthesis, properties, modifications and applications," *Chemical Reviews*, vol. 107, no. 7, pp. 2891–2959, 2007.

[37] N. Al Dahoudi, Q. Zhang, and G. Cao, "Alumina and hafnia ald layers for a niobium-doped titanium oxide photoanode," *International Journal of Photoenergy*, vol. 2012, Article ID 401393, 6 pages, 2012.

[38] V. K. Sharma, K. Winkelmann, Y. Krasnova, C. Lee, and M. Sohn, "Heterogeneous photocatalytic reduction of ferrate(VI) in UV-irradiated titania suspensions: role in enhancing destruction of nitrogen-containing pollutants," *International Journal of Photoenergy*, vol. 5, no. 3, pp. 183–190, 2003.

[39] D. J. Yang, Z. F. Zheng, H. Y. Zhu, H. W. Liu, and X. P. Gao, "Titanate nanofibers as intelligent absorbents for the removal of radioactive ions from water," *Advanced Materials*, vol. 20, no. 14, pp. 2777–2781, 2008.

[40] D. Yang, H. Liu, Z. Zheng et al., "An efficient photocatalyst structure: TiO_2(B) nanofibers with a shell of anatase nanocrystals," *Journal of the American Chemical Society*, vol. 131, no. 49, pp. 17885–17893, 2009.

[41] D. Yang, C. Chen, Z. Zheng et al., "Grafting silica species on anatase surface for visible light photocatalytic activity," *Energy and Environmental Science*, vol. 4, no. 6, pp. 2279–2287, 2011.

[42] D. Yang, S. Sarina, H. Zhu et al., "Capture of radioactive cesium and iodide ions from water by using titanate nanofibers and nanotubes," *Angewandte Chemie—International Edition*, vol. 50, no. 45, pp. 10594–10598, 2011.

[43] H. Yang, S. Zhu, and N. Pan, "Studying the mechanisms of titanium dioxide as ultraviolet-blocking additive for films and fabrics by an improved scheme," *Journal of Applied Polymer Science*, vol. 92, no. 5, pp. 3201–3210, 2004.